Image Reconstruction of a Metal Fill Industrial Process Using Genetic Programming

Alaa Al-Afeef
Information Technology Department
Al-Balqa Applied University (BAU)
Salt, Jordan
alaa.afeef@gmail.com

Alaa F. Sheta
Computers and Systems Department
Electronics Research Institute (ERI)
Cairo, Egypt
asheta66@gmail.com

Adnan Al-Rabea
Information Technology Department
Al-Balqa Applied University (BAU)
Salt, Jordan
adnan_alrabea@yahoo.com

***Abstract*—Electrical Capacitance Tomography (ECT) is one of the most attractive technique for industrial process imaging because of its low construction cost, safety, non-invasiveness, non-intrusiveness, fast data acquisition, simple structure, wide application field and suitability for most kinds of flask and vessels. However, image reconstruction based ECT suffers many limitations. They include the *Soft-field* and *Ill-condition* characteristic of ECT. The basic idea of the ECT for image reconstruction for a metal fill problem is to model the image pixels as a function of the capacitance measurements. Developing this relationship represents a challenge for systems engineering community. In this paper, we presents our innovative idea on solving the non-linear inverse problem for conductive materials of the ECT using Genetic Programming (GP). GP found to be a very efficient algorithm in producing a mathematical model of image pixels in the form of Lisp expression. The reported results are promising.**

***Keywords*-Electrical Capacitance Tomography; Process Tomography; Image Reconstruction; Genetic Programming;**

I. Introduction

Tomography is a method of producing a sectional image (tomogram) of the internal structures of an object (i.e. human body, oil pipeline and others) using wave of energy [1]–[3]. Technically, Tomography involves taking direct sectional images (e.g. X-ray, infrared or Ultrasound tomogram) or reconstructing indirect sectional images using boundary measurements based on the internal characteristics of the monitored object (e.g, Electrical Tomogram) [4].

Different process tomography systems have been built and tested for various process applications [5]. Industrial processes are among those process applications that tend to be complex in nature; however, Tomography is one of the few feedback tools that give information about what is actually happening inside industrial process [6], which is important to 1) Reduce production costs through enhancing efficiencies and better yields; 2) Develop process efficiently; 3) Simplify process and improve products.

A. Electrical Capacitance Tomography (ECT)

ECT is a method evolved since 1980s for determination of the dielectric permittivity distribution in the interior of an object from external capacitance measurements. Thus, the boundary measurements related to the interior characteristics of an object under inspection are used for image reconstruction.

ECT has the advantage of not requiring direct contact between the sensor and the object under inspection (*non-invasive*) and not changing the characteristics of the object being explored (*non-intrusive*) [7]. Moreover, it is a safe method for both human and environment, fast and relatively inexpensive method compared to hard field tomography.

ECT has been applied to study various industrial processes using capacitance measurements to form images. For example: gas/liquid flows [8], pneumatic conveying process [9], water/oil/gas separation process [10], fluidized beds [11] and determining the characteristic of the molten metal in Lost Foam Casting (LFC) process [12], [13] and many others.

B. ECT Sensor Array

Capacitance sensor consists of several electrodes (i.e. capacitive plates) located on the periphery of the process vessel. For a Twelve-electrode sensor system, electrodes 1 to 12 are used as source electrodes, one at the time. When one electrode is fired (with electrical current), 11 capacitance detectors are used simultaneously to measure the capacitance between the source and the remaining electrodes. With N electrode, $\frac{N(N-1)}{2}$ independent capacitance measurements can be acquired. The capacitance measurements are then used to reconstruct the dielectric permittivity distribution using a reconstructing algorithm. The result is usually presented as a visual image, and hence this process is denoted as *image reconstruction* [3], [14].

C. What Makes ECT a Challenging Problem?

There are few problems make the implementation of ECT system a challenge [5], [7]. The reasons are given [7], [15] as follows:

1) *Soft fields* affect the sensors measurements in which the electric field lines are dependent on the permittivity distribution in the imaging domain (i.e. the distortion of electro-magnetic field is caused by the material permittivity) [5], [16].
2) *Ill-condition* of the ECT problem means ill-posed response of the sensor at different locations in the

978-1-4244-8136-1/10/$26.00

imaging domain (i.e., the sensitivity nears the wall is very high unlike the sensitivity nears the center which, is very low).

3) *The limited number of independent measurement* affects the process of developing an outstanding images [5].
4) *Ill-posed* of the ECT problem. ECT system is considered an underdetermined system since the number of unknowns in the system (i.e. image pixels) is more than the number of knows (i.e. capacitance measurements) [17].
5) *Non-linearity* of the relationship between the measured capacitance and permittivity distribution exists [3], [5], [6], [18]; Furthermore, it is hard to establish an analytical and explicit expression which describes this relationship.

In order to improve the imaging accuracy, one may 1) increase the number of measurements by increasing the number of electrodes; 2) improve the reconstruction algorithm so that more information can be extracted from the captured data, however, increasing the number of electrodes has a limited impact on the imaging accuracy improvement [19]. This means that, in order to improve the reconstructed image, more accurate reconstruction algorithms must be developed [3], [12].

II. ECT Computational Problems

There are two major computational problems in ECT image reconstruction [20]. They are:

1) *The forward problem* in which the capacitance measurement C_{ij} between electrodes i and j need to be determined from the permittivity distribution $\varepsilon(x, y)$ as given in Equation (1).

$$C_{ij} = F(\varepsilon(x, y)). \tag{1}$$

2) *The inverse problem* which is the process of finding the inverse relationship such that, the permittivity distribution is estimated using capacitance measurements and (as a result) constructing a visual image using a reconstructing algorithm. This process is also called *image reconstruction process*. The inverse relationship can be expressed as in Equation (2).

$$\varepsilon(x, y) = F^{-1}(C_{12}, C_{13}, C_{14}, ..., C_{ij}, ..., C_{N-1,N}) \tag{2}$$

III. Genetic Programming

Genetic programming (GP) is is an evolutionary computation (EC) technique that automatically search for an optimal solution of a problem without requiring the user to know or specify the form or structure of the solution in advance. At the most abstract level GP is a systematic, domain-independent method for getting computers to solve problems automatically starting from a high-level statement of what needs to be done [21]. GP has been successfully applied to solve large number of difficult problems such as modeling of industrial processes [22], [23], forecasting of river flow [24] and image reconstruction [3].

A. Trees Based GP

In Trees Based GP, the individual, also called *chromosome*, is represented as a variable sized tree structure. This type of representation allows a variety of models to be developed. A tree consists of nodes and terminals. In every terminal node, there is an operand and in every node there is a function. Trees can be easily evaluated in a recursive manner. This way we can evolve mathematical models in a very simple way such as in programming using Lisp language [25]. Such a representation is simple and has been used frequently for the data classification and modeling problems. A simple tree structure can be presented in Figure (1) as described in Equation (3).

$$y = x_1 * x_2 + x_1 \tag{3}$$

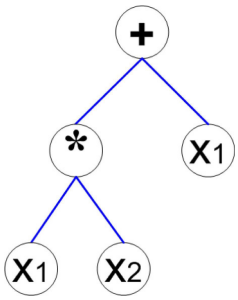

Figure 1. Example of GP tree structure

B. Preparatory steps of genetic programming

Before applying GP, four major preparatory steps need to be specified [21]:

1) The Definition of the function and terminal set (primitive set) for a particular problem.
2) Fitness measure for the problem. This specifies what needs to be done.
3) The control parameters for the run (for example, population size, max generations and maximum tree depth).
4) The termination criterion which may include a maximum number of generations to be run as well as a problem-specific optimum solution.

C. Evolutionary Process of GP

The evolutionary processes of GP starts by executing each program *individual* in the randomly created initial population and calculating its fitness using the problem-specific fitness measure. While termination criterion is not yet reached we do the following [21]:

- Select one or two program (i.e. parent individual) from the population using a selection mechanisms (i.e. tournament, rank, etc.).
- Create an offspring (child individual) using crossover, mutation, reproduction and architecture-altering operators.
- Compute the new generation. This process will end when the termination criterion is satisfied.

The best-so-far individual is typically designated as the result of the run.

D. Genetic Operators

1) Reproduction: Reproduction is the process that selects individuals according to their fittest, in order to copy them into the next generation [21]. The objective of reproduction is to keep good individuals and have good genetic material in the population.

2) Crossover: Crossover is applied on individuals by simply switching one of its nodes (i.e. branch) with another node from another individual in the population [21]. The objective of crossover is to exploit the genetic material in a population.

3) Mutation: Mutation affects an individual in the population. It can replace a whole branch in the selected individual, or it can replace just distinct node [21]. The objective of mutation is to introduce new genetic material to an existing individual.

4) Architecture-Altering: Architecture-altering operations are set of transformations that can alters the architecture of a tree by creating, modifying or deleting program structures during a genetic programming run [26]. The objective of Architecture-altering is to alter the underlying architecture of the program instead of simply modifying function and argument calls.

IV. Proposed GP Model

Our objective is to find a GP Inverse Solver that Mathematically describes the nonlinear relationship F between the capacitance input variables C and the image pixel P of Image vector G that represents the distribution of metal in the imaging area, as given in Equation (4).

$$G_p = F(C_1, C_2, ..., C_{\frac{N(N-1)}{2}}) \quad (4)$$

In our case presented, the inverse solver consists of 64 GP Models. Each model is responsible for deriving a relationship between capacitance measurements $[C_1 - C_{66}]$ and a specific pixel in an ECT image of 64 pixels. In Figure (2), the structure of the proposed system is shown. The number of measurements is 66 representing all the unique combinations of measurements between 12 electrodes distributed around the measuring area. These measurements are represented by the symbols $C_1, ..., C_{66}$. All the measurements are then presented to each system of the 64 GP systems, one at a time. The GP systems are constructed using Lilgp tool [27].

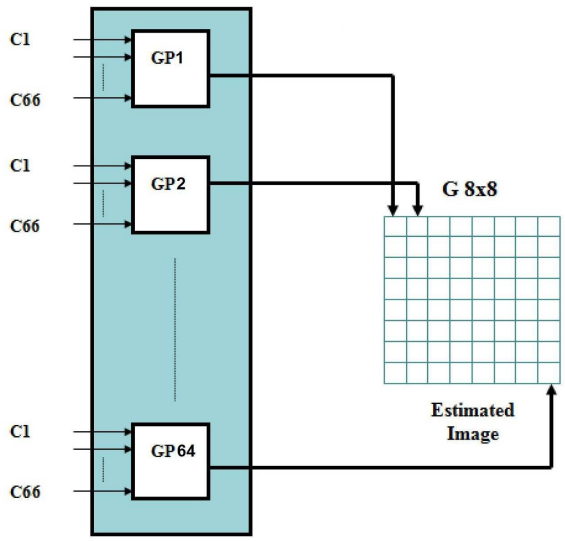

Figure 2. Proposed GP Inverse Solver Model

V. Experimental Setup

A. Data Generation for Lost Foam Casting (LFC)

LFC is a casting process that uses foam patterns as molds in which the molten metal decomposes the foam pattern and creates a casting in its shape [12], [18]. LFC is among those applications that use the ECT technique to express the metal fill profile. A better understanding of the characteristics of the molten metal in the foam pattern is important to reduce the fill related defects and to improve the final casting [12].

Training data are originated as frames using finite element ANSYS software package [28] to simulate the properties of the molten metal inside the foam patterns during the casting process. The metal starts melting down at the casting gate and grows. Every single frame represents the metal distribution at distinct time as in Figure (3) and (4) [18].

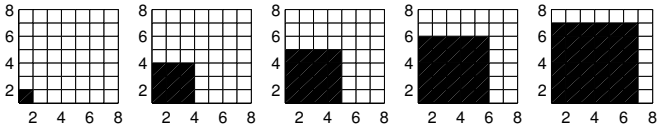

Figure 3. ANSYS generated ECT images of single point of metal fills

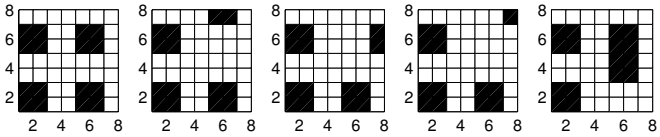

Figure 4. ANSYS generated ECT images of multi point of metal fills

B. GP Control parameters

Control parameters for GP are shown in Table II with a default breeding parameters as presented in [21]. The GP experiment setup for Modeling metal fill distribution in Lost Foam Casting Problem is give in Table I.

Table I
GP EXPERIMENT SETUP

Objective	Find a function of 66 independent variable (capacitance measurements) and one dependent variable (image pixel), in symbolic form, that fits a given Training sample of the form $(C_1, C_2, ..., C_{66} : G_i)$ data points.
Terminal set	$C_1, C_2, ..., C_{66}$ (the independent variables).
Function set	+, -, *
Fitness criteria	In a given sample of training data points $(C_1, C_2, ..., C_{66} : G_i)$. The fitness is the absolute difference between the dependent variable produced by the GP and the target value Gi of the dependent variable. $(\|G_i^{Original} - G_i^{GP-Estimated}\|)$.
Raw fitness	The sum taken over the fitness cases (fc) $(\sum_{i=1}^{fc} G_i^{Original} - G_i^{Estimated})$
Standardized fitness	Equals raw fitness divided by the count of fitness cases.
Hits	Number of fitness cases for which the value of the dependent variable produced by the GP comes within 0.001 of the target value G_i of the dependent variable.

Table II
GP CONTROL PARAMETERS FOR MODELING METAL FILL DISTRIBUTION

Parameter	**Value**
Population size	30000
Maximum number of generations to be run	100
Probability of crossover	90 %
Probability of reproduction	10 %
Maximum size for S-expressions created in the run	17
Maximum size for initial random S-expressions	6
Probability of mutation	0 %
Probability of permutation	0 %
Initial random population generating method	half and half
Selection method	tournament, size=7
Adjusted fitness	used
Over selection	not used

C. Fitness Function

The fitness function selected to develop the 64 GP models was defined as the error percentage for the developed models. The EP is given in Equation (5).

$$EP_{set} = \frac{G^{set} - OAE}{G^{set}}, where \quad (5)$$

$$OAE = \sum^{\alpha}\sum^{\beta} \left|G^{Actual} - G^{Estimated}\right|$$

where set is either the training or testing set of experiment. EP is the error percentage of a given set. G^{set} is the total number of pixels of all images in that set. Overall absolute error (OAE) is the summation of the absolute difference between the actual and the GP estimated image pixels of all images in the set. α is total number of images in the set. β represents the image-size (i.e. the total number of pixel in a single image in the experiment). G^{Actual} and $G^{Estimated}$ are the actual and estimated pixel, respectively.

VI. EXPERIMENTAL RESULT

In this section we explored the modeling metal fill distribution in Lost Foam Casting Problem. The proposed GP process that was explained is utilized using the setting in Table II to create a GP Models that solve the inverse problem for metal fill.

For our experimentation, we have used Lilgp1.1 [27] software system written in C language to produce our results. Lilgp is well-known software known to be fast, memory effcient and well documented tool which provide several features not typically found in other GP systems, such as the support of parallel processing.

Two cases of an ANSYS generated examples for metal fill distribution in Lost Foam Casting Problem were considered. The first case involves Single Metal Filling Points images as given in Figure (3). The second case include multi Metal Filling points images as given in Figure (4). A distinct set of those examples were not presented to the GP system during the training phase. These sets were used for testing the performance of the GP Inverse Solver. The computation time was approximately one month for each experiment to finish the run. A personal computer with 32-bit Operating System, CPU Core2Duo, 2.0 GHz, and RAM Memory of 2GB was used to provide the required models.

In the Single Metal Filling case, a Training set of 268 single fill ECT images with the corresponding capacitance measurements was provided to the GP system. A Testing set of size 67 was used for testing the performance of the GP Models. A subset of these patterns and their corresponding GP estimated patterns are shown Figure (5).

The original ECT images are represented in binary format whiles the GP estimated ones are in grayscale format, therefore, a transformation might be needed to transform grayscale images into binary ones. In order to accomplish that, an optimum threshold level must be found to be used in the transformation process. The choice of the optimal threshold is done by considering only the training set since the testing set has not to be involved in any phase of the system design and tuning, it is used only to evaluate its actual performance in a condition similare to the normal operation.

Figure (7) shows a plot of every threshold level and their corresponding overall Absolute Error. The Best-so-far curve of this case is shown in Figure (6).

The error percentage for the developed single and multi point of fill experiments is given in Table III, Table IV

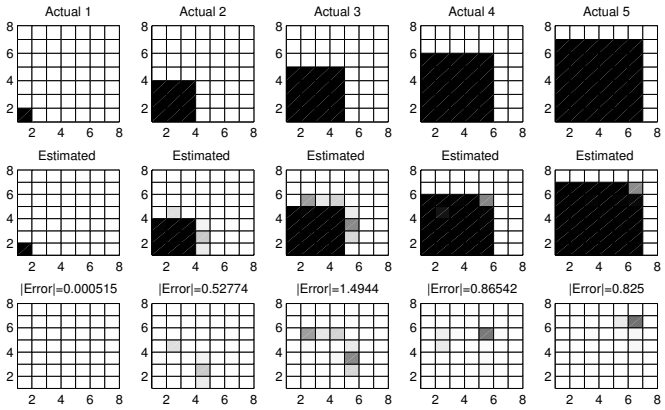

Figure 5. Examples for actual and estimated patterns using GP Modeling with single filling - (1-3) Training Cases, (4-5) Testing Cases

respectively and is calculated according to Equation (5).

Table III
ERROR PERCENTAGE FOR THE SINGLE FILLING IMAGES

	GP estimated Images	Thresholded GP Images, level=0.41
Training Case	0.0253 %	0.0110 %
Testing Case	0.0263 %	0.0103 %

Table IV
ERROR PERCENTAGE FOR THE MULTI FILLING IMAGES

	GP estimated Images	Thresholded GP Images, level=0.03
Training Case	0.0014	0.0
Testing Case	0.0016	0.0

Equation (6) shows an example of the GP function which is obtained through the application of the Genetic Programming. In this model, It was found that G_{64} is mostly affected by the measurements C_{54}, C_{46}, C_{52}, C_{24} and C_{54}. The values of the input variables (i.e C_s) is in the range: $1 \geq C \geq 0$. This is what makes the values of G does not exceeds a range of: $1 \geq G \geq -1$ which is mapped using threshold level into $\{1, 0\}$.

$$G_{64} = C_{54} * C_{46}^{3}(C_{46}^{38} * C_{52}^{4} * C_{54} - C_{24} * C_{46}^{18} * C_{52}^{2} - C_{54}) \quad (6)$$

where G_{64} is the estimated pixel number 64 of image G, C is the corresponding capacitance measurement.

VII. CONCLUSIONS AND FUTURE WORK

In this paper, a new technique for solving the non-linear inverse problem of electrical capacitance tomography has been introduced. The proposed technique is based on the use of Genetic programming to identify the models that relating the sensors' capacitance measurements to the permittivity distributions. The modeling process is described and the estimated models are validated for the case of single filling point. The solution showed promising results in terms of the accuracy, the quality of reconstructed image, as well as the convergence rate. The main limitation of this technique is that the convergence process based GP is time consuming. also, sufficient training data is needed. We plan to investigate other metal distributions processes in order to improve the reconstructed images and apply genetic programming to solve the forward problem of ECT.

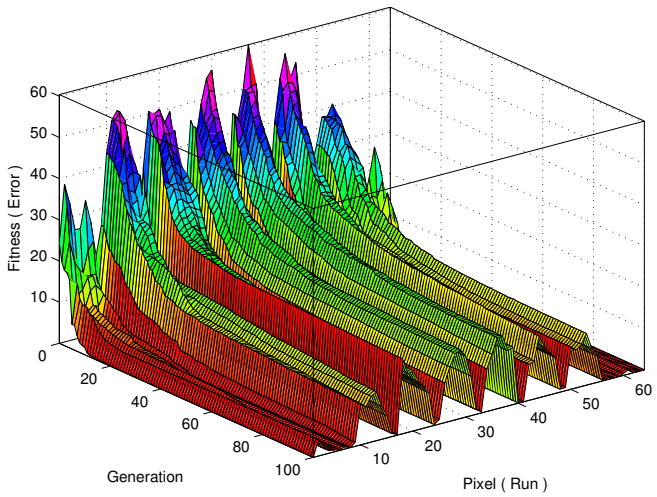

Figure 6. Best-so-far curves for the single point of metal fills Experiment

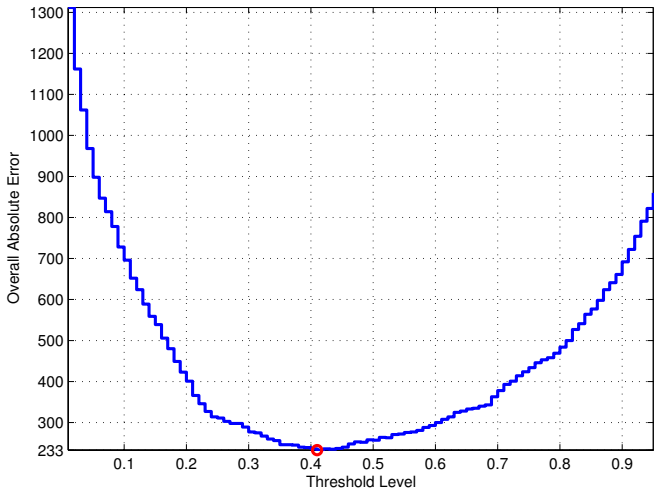

Figure 7. Distribution of the OAE and the corresponding thresholding levels

ACKNOWLEDGMENT

ANSYS Data for Lost Foam Casting was provided by Drs. Mohamed Abdelrahman and Wael Deabes, Tennessee Technological University. Data was produced in conjunction with research project GO14228 supported by US Department of Energy (DOE), USA.

REFERENCES

[1] M.S. Beck and R.A. Williams. Process tomography: a european innovation and its applications. *Measurement Science and Technology*, 7(3):215–224, 1996.

[2] B. Hoyle. Process tomography using ultrasonic sensors. *Measurement Science and Technology*, 7(3):272–280, 1996.

[3] Alaa. S. Al-Afeef. Image reconstructing in electrical capacitance tomography of manufacturing processes using genetic programming. Master's thesis, Al-Balqa Applied University, July 2010.

[4] S. Gehrke and K.E. Wirth. Application of conventional- and dual-energy x-ray tomography in process engineering. *Sensors Journal, IEEE*, 5(2):183– 187, April 2005.

[5] O. Isaksen. A review of reconstruction techniques for capacitance tomography. *Sensors Journal, IEEE*, 7(3):325–337, March 1996.

[6] Q. Marashdeh, W. Warsito, L.S. Fan, and F. L. Teixeira. A nonlinear image reconstruction technique for ect using a combined neural network approach. *Measurement Science and Technology*, 17(8):20972103, August 2006.

[7] J. Lei, S. Liu, Z. Li, and M. Sun. Image reconstruction algorithm based on the extended regularised total least squares method for electrical capacitance tomography. *IET Science, Measurement and Technology*, 2(5):326336, September 2008.

[8] R. White. Using electrical capacitance tomography to monitor gas voids in a packed bed of solids. *Measurement Science and Technology*, 13(12):1842–1847, December 2002.

[9] K. Brodowicz, L. Maryniak, and T. Diakowski. Application of capacitance tomography for pneumatic conveying processes. In *Proc. 1st ECAPT Conf. (European Concerted Action on Process Tomography)*, page 2629, Manchester, March 1992.

[10] O. Isaksen, A.S. Dico, and E.A. Hammer. A capacitance-based tomography system for interface measurement in separation vessels. *Measurement Science and Technology*, 5(10):1262–1271, October 1994.

[11] G.E. Fasching and N.S. Smith. A capacitance imaging for three dimensional imaging of fluidised beds. *Rev. Sci. Instrum*, 62:2243–2251, 1991.

[12] M. Abdelrahman, Alaa Sheta, and Wael Deabes. Fuzzy mathematical modeling for reconstructing images in ect of manufacturing processes. In *Proc. Fuzzy Mathematical Modeling for Reconstructing Images in ECT of Manufacturing Processes*, December 2009.

[13] W.A. Deabes and M.A. Abdelrahman. Solution of the forward problem of electric capacitance tomography of conductive materials. In *The 13th World Multi-Conference on Systemics, Cybernetics and Informatics: WMSCI*, Orlando, Florida, USA, July 2009.

[14] Manuchehr Soleimani and William R B Lionheart. Nonlinear image reconstruction for electrical capacitance tomography using experimental data. *Measurement Science and Technology*, 16(10):1987, 2005.

[15] H. Yeung and A. Ibrahim. Sensor response data base in multiphase flows. *Journal of Flow Measurement and Instrumentation*, 14::219223, August 2003.

[16] Chen Yao, Wang Xiaowei, and Jiangyan. Study on image reconstruction algorithm for electrical capacitance tomography system. In *HIS '09: Proceedings of the 2009 Ninth International Conference on Hybrid Intelligent Systems*, pages 480–483, Washington, DC, USA, 2009. IEEE Computer Society.

[17] S.M. Hoyle, B.S. Thorn, C. Lenn, C.G. Xie, S.M Huang, and M.S. Beck. Electrical capacitance tomography for flow imaging system model for development of image reconstruction algorithms and design of primary sensor. In *IEEE Proceedings G 139*, page 8998, 1992.

[18] M. Abdelrahman, Jeanison Pradeep Arulananthama, Ralph Dinwiddieb, Graham Walfordc, and Fred Vondraa. Monitoring metalfill in a lost foam casting process. *ISA Transactions*, 45(4):459–475, 2006.

[19] O. Isaksen and J.E. Nordtvedt. An implicit model based reconstruction algorithm for use with a capacitance tomography system reviewed proc. In *3rd ECAPT Conf. (European Concerted Action on Process Tomography)*, page 21526, March 1994.

[20] K. Alme and S. Mylvaganam. Electrical capacitance tomographysensor models, design, simulations, and experimental verification. *IEEE SENSORS*, 6(5), OCTOBER 2006.

[21] John R. Koza. *Genetic Programming: On the Programming of Computers by Means of Natural Selection*. MIT Press, 1992.

[22] A. Hussian, A. Sheta, M. Kamel, M. Telbany, and A. Abdelwahab. Modeling of a winding machine using genetic programming. In *Proceedings of the Congress on Evolutionary Computation (CEC2000)*, pages 398–402, 2000.

[23] A. Sheta and J. Gertler. Modeling the dynamics of an automotive engine using genetic programming. In *Proceedings of the International Symposium on Engineering of Natural and Artificial Intelligent Systems (ENAIS2001), American University in Dubai, U.A.E.*, 2000.

[24] A. Sheta and A. Mahmoud. Forecasting using genetic programming. In *Proceedings of the 33 rd Southern Symposium on System Theory, March 19-20, Athens, Ohio, USA*, pages 343–347, 2001.

[25] Stuart C. Shapiro (Editor). *Encyclopedia of Artificial Intelligence*. John Wiley, 2 edition, January 1992. 1792 pages.

[26] John R. Koza, David Andre, Forrest H Bennett III, and Martin Keane. *Genetic Programming 3: Darwinian Invention and Problem Solving*. Morgan Kaufman, April 1999.

[27] Douglas Zongker and Bill Punch. lilgp 1.01 user's manual. Technical report, Michigan State University, USA, 26 March 1996.

[28] Y. Nakasone, T. A . Stolarski, and S. Yoshimoto. *Engineering analysis with ANSYS software*. A Butterworth-Heinemann Title, December 2006. ISBN:075066875X.